Pure Appl. Chem., Vol. 82, No. 11, pp. 2157–2165, 2010.
doi:10.1351/PAC-CON-09-11-35

Pyrolytic carbons from acid/base-treated rice husk as lithium-insertion anode materials*

George Ting-Kuo Fey[1,‡], Yung-Da Cho[1], Chung-Lai Chen[1], Yu-Yen Lin[1], T. Prem Kumar[2], and Shih-Hung Chan[3]

[1]Department of Chemical and Materials Engineering, National Central University, Chung-Li 32054, Taiwan; [2]Central Electrochemical Research Institute, Karaikudi 630 006, Tamil Nadu, India; [3]Fuel Cell Center, Yuan Ze University, No. 135, Yuandong Road, Chung-Li, Taoyuan 32003, Taiwan

Abstract: The effects of hydrochloric acid and sodium hydroxide as leachants on the lithium-insertion properties of pyrolytic carbons prepared from rice husk are presented. All the disordered carbonaceous products had interlayer spacings (d_{002}) of more than 3.7 Å, with values decreasing with an increase in the concentration of the leachant. The values of the H/C ratio and the *R*-parameter, the reciprocal of which is a measure of the number of non-parallel single layers of carbon, also diminished with an increase in the concentration of NaOH. An increase in the alkali concentration was found to improve the porosity of the carbons, as evidenced by the Brunauer–Emmett–Teller (BET) surface area data. An interaction of these factors determines the observed capacities of the carbon products. The highest insertion and deinsertion capacities were observed with the carbon obtained from rice husk treated with 0.3 M NaOH, the values being 819 and 463 mAh/g, respectively.

Keywords: anode materials; carbon; lithium-ion batteries; rice husk leaching; rice husk pyrolysis.

INTRODUCTION

Buoyed by successive improvements in the safety and performance of carbon anode-based lithium-ion batteries, more attention is being focused worldwide on developing novel carbonaceous materials and other nanostructured anode materials [1–3] with superior characteristics. Of particular interest are disordered carbons, prepared by the pyrolysis of organic precursors that are able to store large amounts of lithium, typically more than 400 mAh g^{-1} [4–8]. The high lithium capacities of these carbons have been attributed to crystallographic disorder and hydrogen content. Such carbonaceous materials are generally obtained by the pyrolysis of organic precursors at temperatures between 600 and 1000 °C. Natural biomass materials such as rice husk [9], cotton [10], wood [11], peanut kernel [12], walnut and almond shells [13], and sugar [14–17] have been exploited as precursors for the production of pyrolytic carbons. Pyrolytic carbons with different electrochemical characteristics can be obtained by varying the nature of the precursor and the pyrolysis conditions. The resulting macromolecular structure of these disordered carbons is maintained during heat treatment and only loses small molecules by degradation and develops even more cross-linking so that fusion cannot take place. The loss of small molecules and the

*Paper based on a presentation at the 5th International Symposium on Novel Materials and Their Synthesis (NMS-V) and the 19th International Symposium on Fine Chemistry and Functional Polymers (FCFP-XIX), 18–22 October 2009, Shanghai, China. Other presentations are published in this issue, pp. 1975–2229.

‡Corresponding author: Tel.: +886-3-422-7151-34206 or 886-3-425-7325; Fax: +886-3-425-7325; E-mail: gfey@cc.ncu.edu.tw

retention of the complex macromolecular structure lead to high microporosity, with surface areas in the order of 1000 $m^2\ g^{-1}$.

Carbon prepared at low temperatures is amorphous or disordered, consisting of graphitic crystallites and disordered areas with large internal pore volume and surface area. Several models have been proposed to describe its structure [18–21]. The mechanisms of lithium storage in these carbons have been reviewed [22]. The graphitic crystallite areas are a few orderly stacked graphene molecules that can store lithium like graphite, while the disordered areas include micropores, tetrahedral carbon atoms, carbon chains, etc., which are also a part of graphene molecules. As a result, the greater the graphitic crystallite areas, the higher the discharge capacity. Around the micropores, there are imperfect carbon structures, including carbon radicals that present an electron paramagnetic resonance (EPR) response [22–25]. When lithium intercalates into graphite or crystallites, the intensity of the EPR signal will increase due to the spin-orbit interaction between σ-spin of the intercalated lithium and π-electrons in the grapheme molecule [22]. The complicated macromolecular structures of disordered carbons with high surface area, high microporosity, and hydrogen content result in high lithium capacities of these carbons.

Despite the advantage of high lithium capacity, the disordered carbons suffer from a significant loss in initial capacity. The irreversible capacity of graphitic carbons is mainly due to passivation and exfoliation [26]. The passivation of graphitic carbons related to the electrochemically active surface area is derived from electrolyte instability, which causes a layer of lithium compounds to form at a low potential (about 0.8 V vs. Li^+/Li), with an irreversible capacity loss of less than 50 mAh g^{-1} [26]. The exfoliation of graphitic carbons related to the rhombohedral phase content is attributed to the intercalation of solvated lithium ions between graphene sheets before passivating layer formation is complete, resulting in an irreversible capacity loss up to 1000 mAh g^{-1} [26]. The loss of irreversible capacity in the low-voltage plateau region is related to water adsorption on the surface of the carbon, as evidenced by the ethylene surface treatment [27] and dewatering temperature experiments [28]. Lithium insertion in carbons prepared from organic precursors heated from 500 to 1100 °C often showed large hysteresis [29,30]. This phenomenon was the result of interaction between the inserted lithium atoms with neighboring hydrogen-terminated edges of hexagonal carbon fragments, causing a change in the bond from sp^2 to sp^3. The level of hysteresis seemed to be proportional to the hydrogen content of the carbon samples [31]. Carbons pyrolyzed below 800 °C contained substantial hydrogen (H/C atomic ratio > 0.1), whereas carbons heat-treated to near 1000 °C contained much less hydrogen (H/C atomic ratio < 0.05) [29].

The surface and structural characteristics of carbon electrodes affect the kinetics and reversibility of the electrochemical processes. Taking this into consideration, carbon materials have been subjected to a variety of physical and chemical treatments, effecting changes in the surface functional groups, morphology, and even crystallographic parameters. Chemical activation is a well-known method for preparing activated carbons because it can use lower temperatures for pyrolysis, obtain very high surface area and micropore volume particles, and produce a much higher yield than physical activation. The generation of pores in these materials is dictated by the nature of the precursor and the chemical etching agent. The etching process removes carbon atoms to open up closed pores and enlarge existing ones. In an earlier communication [9], we presented our results on the lithium-insertion properties of rice husk-derived carbons. We showed that these disordered carbons maintained good reversibility upon repeated cycling, the first- and fifth-cycle deinsertion capacities being 1055 and 1051 mAh g^{-1}, respectively [9]. In this paper, we report the structural and lithium-insertion properties of carbons derived by the carbonization of HCl/NaOH-treated rice husk.

EXPERIMENTAL

Rice husk from a local source was thoroughly washed and dried. The dried husk was refluxed with an excess of 1.0, 3.0, or 6.0 M HCl for 1 h, cooled to room temperature, washed free of acid with distilled

water, and dried. A known weight of the refluxed and dried husk was heated in a quartz tube reactor in flowing argon at 150 °C for 1 h (heating rate: 10 °C/min), followed by a 1-h calcination at 700 °C (heating rate: 5 °C/min). The carbon product was ground to a fine powder. The yield of carbon obtained by the HCl treatment was 44 %. The pyrolysis temperature was fixed at 700 °C based on our earlier studies [9]. Treatment with NaOH was carried out as follows. Cleaned and dried rice husk was refluxed with an excess of NaOH (0.01, 0.1, 0.3, 4.0, and 9.0 M) for 1 h, after which it was treated with 3.0 M HCl and carbonized according to the acid-treatment procedure described above. The carbon yield in this case was 26 %. The carbons in this study are designated C-H-X or C-N-X, where H and N stand for HCl and NaOH treatment, respectively, and the X for the molarity of the leachant solution.

Elemental analysis was carried out on a Perkin Elmer CHN 2400 elemental analyzer. Powder X-ray diffractometry was performed (Siemens D 5000 MacScience MXP 18 X-ray diffractometer) with nickel-filtered Cu K_α radiation. The data were collected between scattering angles (2θ) of 5º and 80º in steps of 0.05º. BET surface area measurements were carried out on a Micrometrics ASAP 2010 surface area analyzer. Coin cells of the 2032 configuration were assembled as described earlier [9]. Galvanostatic charge–discharge profiles were recorded between 3.000 and 0.005 V at a 0.1 C-rate on a Maccor Series 4000 multi-channel battery tester.

RESULTS AND DISCUSSION

Structural and elemental analyses

Effect of HCl treatment

Refluxing rice husk with HCl results in the reduction of cellulose, which forms the main body of the husk [32]. Simultaneously, the proteins in the rice husk are broken into amino acids, and the cellulose with large molecular weight is leached out as low-molecular-weight compounds [33]. The result is a porous, high-purity product, which is carbonized after pyrolysis, with an attendant loss of H_2O, CO_2, and CH_4. The evolution of gases results in a further development of porosity. For example, the surface area of the C-H-3.0 was 277 $m^2\ g^{-1}$ [9].

The X-ray diffraction patterns recorded for the carbon materials prepared with different concentrations of HCl are shown in Fig. 1. The diffraction patterns show broad, but weak (002) reflections, indicating their disordered nature. The (002) reflections indicate small islands of coherent and parallel stacked graphene sheets. It is known that pyrolytic carbons prepared at temperatures below 1000 °C have a high degree of turbostratic disorder, with a random stacking of hexagonal graphene layers and unorganized carbons [34,35]. The unorganized carbons are comprised of tetrahedrally bonded carbons or highly buckled graphene sheets placed between turbostratic structural regions. The average layer spacing, d_{002}, was found to be consistently higher than the 3.345 Å observed in perfectly graphitic structures (Table 1). The inter-layer spacing was found to be the greatest for C-H-3.0 (3.964 Å). It is suggested that a HCl concentration of 3.0 M was optimal for the leaching process.

Table 1 Crystallographic parameters, elemental analytical data, and surface areas of carbons derived from HCl-derived rice husk.

HCl Conc. (M)	d_{002} (Å)	*R*-parameter	Composition (wt %)			H/C	Surface area ($m^2\ g^{-1}$)
			C	H	N		
1.0	3.938	2.54	51.03	1.83	0.46	0.43	201
3.0	3.964	2.02	47.12	1.88	1.03	0.48	277
6.0	3.717	2.58	50.33	1.82	0.28	0.43	173

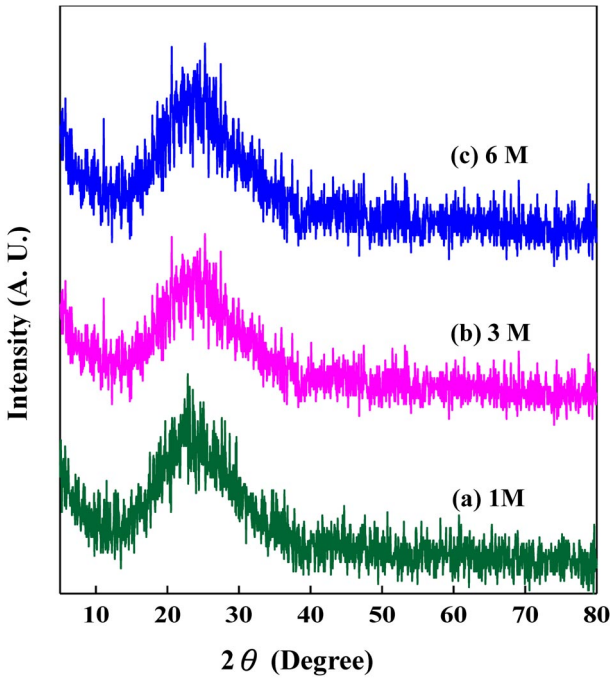

Fig. 1 X-ray diffraction patterns of pyrolytic carbons derived from HCl-derived rice husk.

Rice husk is rich in SiO_2, as can be seen from the high content (87–97 %) of silica in the ash obtained after burn-off [36]. Krishnarao and Mahajan [32], who studied the effect of HCl treatment prior to the pyrolysis of rice husk, reported that above 1300 °C, the formation of SiC whiskers was a dominant process. Although the pyrolysis process is accompanied by graphitization of the carbon matrix, crystallization of amorphous silica and generation of SiC [37], our pyrolysis temperature (700 °C) was too low to generate crystalline SiO_2 or SiC detectable by X-ray diffraction.

Dahn et al. [38,39], who investigated the electrochemical insertion of lithium into disordered carbons, established a correlation between the electrochemical behavior and a derived parameter called the *R*-parameter, defined as the ratio of the intensity of the (002) X-ray diffraction peak to that of the diffuse background. The reciprocal of this parameter is a semi-quantitative measure of the number of carbon atoms present in unorganized graphene layers in the carbon sample. The *R*-parameters calculated for the carbon samples derived from acid-leached rice husk are listed in Table 1. It can be seen that the *R*-parameter is the lowest for C-H-3.0. The low value indicates that the number of unorganized graphene layers was high for this product. In other words, this carbon had the smallest parallel stacking of graphene sheets among the three carbons studied. Together with the fact that the d_{002} value for this carbon was the highest, this indicates that the concentration of the leachant has a definite effect on the product characteristics.

Pyrolytic carbons prepared at temperatures below 1000 °C are known to retain small amounts of heteroatoms such as hydrogen, oxygen, and nitrogen present in the precursor molecule [40]. The H/C ratio of the C-H-3.0 carbon was 0.48, which is rather large (Table 1). The hydrogen content has a direct impact on the lithium-insertion behavior of the carbon. The unaccounted part of the pyrolysis products is ascribed to oxygen, present in carbons as oxygen-containing functional groups.

Effect of NaOH treatment

NaOH as a chemical agent for pore generation in carbonaceous materials is scarcely found in the literature [41–44] despite its apparent advantages over the commonly employed KOH, which is expensive

and more corrosive. In this study, NaOH was used for the treatment of the husk prior to carbonization, so that the precursor material was already porous. The NaOH treatment should result in leaching away silica from the husk, with the production of sodium silicate. In the subsequent calcination step, the evolving gases develop the carbonization product into a porous matrix. From Table 2, it can be seen that the surface areas of C-N-0.01 and C-N-0.1 were 253 and 267 $m^2\ g^{-1}$, which are comparable to the areas of the products obtained by HCl treatment alone. However, there was a remarkable increase in the surface area when the NaOH concentration was increased to 0.3, 4.0, and 9.0 M (Table 2). The increased porosity in the latter cases can be attributed to the vigorous leaching reaction at the higher alkali concentrations.

Table 2 Crystallographic parameters, elemental analytical data, and surface areas of carbons derived from NaOH-derived rice husk.

NaOH Conc. (M)	d_{002} (Å)	*R*-parameter	Composition (wt %)			H/C	Surface area ($m^2\ g^{-1}$)
			C	H	N		
0.01	3.982	2.46	53.25	2.03	0.82	0.46	253
0.1	3.855	1.96	54.16	2.07	0.88	0.46	267
0.3	3.813	1.88	87.56	2.50	1.18	0.34	371
4.0	3.803	1.86	86.95	2.22	0.74	0.32	404
9.0	3.786	1.96	86.45	2.30	0.74	0.31	426

Figure 2 shows the X-ray diffraction patterns of carbons prepared by the pyrolysis of NaOH-treated rice husk. The diffraction patterns show weak (002) reflections that indicate their disordered nature, although the intensities are lower than those for carbons derived from HCl-treated rice husk. The reduced intensities may be the result of the finely divided nature of the former carbons, as well as the large number of single layers of carbon in them. The larger number of single-layer carbons is reflected

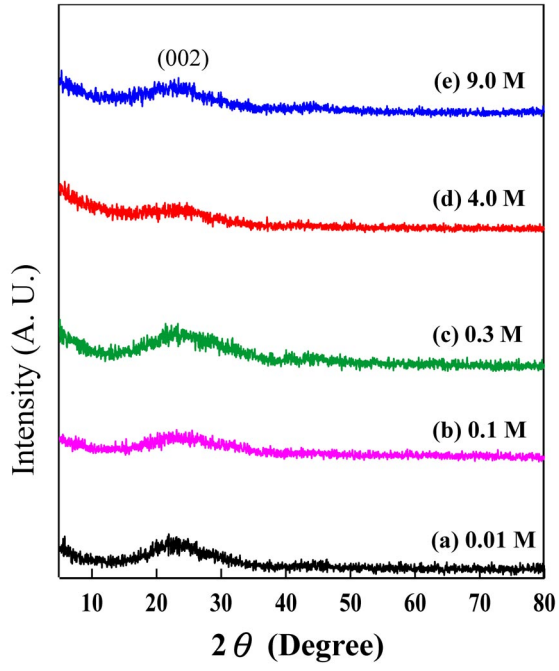

Fig. 2 X-ray diffraction patterns of pyrolytic carbons derived from NaOH-derived rice husk.

in the lower values for the *R*-parameter (Table 2) compared to those for the carbons derived from acid-treated rice husk (Table 1). It can also be seen that the *R*-parameter decreased with NaOH concentration, although it slightly increased when the concentration was raised to 9.0 M. Thus, in general, the number of unparallel single layers of carbon increases with the alkali concentration.

The average layer spacing decreased with an increase in alkali concentration (Table 2). Although the decrease in the inter-layer spacing with NaOH concentration indicated the formation of a more graphitic material, the *R*-parameter values indicated a more disordered nature. It is possible that the increased ordering of the layers is partially camouflaged by the increased porosity of the carbons, as reflected in their surface areas. The enhanced graphitization of the products was also seen in the increased amount of carbon in the products and lower H/C ratio as NaOH concentration was increased.

Charge–discharge studies

The charge–discharge behavior of the carbons derived from HCl-treated rice husk over the first 10 cycles is presented in Fig. 3. The first-cycle lithium-insertion and -deinsertion capacities were, respectively, 524 and 291 mAh g^{-1} (C-H-1.0); 691 and 320 mAh g^{-1} (C-H-3.0); and 428 and 168 mAh g^{-1} (C-H-6.0). The corresponding irreversible capacities were 58, 54, and 61 %. However, the capacities fell drastically as the cycling continued. For example, the 10^{th}-cycle deinsertion capacities of C-H-1.0, C-H-3.0, and C-H-6.0 were 183, 279, and 128 mAh g^{-1}, respectively. However, it must be noted that the coulombic efficiencies for the respective carbons improved from 42, 46, and 39 % in the first cycle to 98, 97, and 98 % in the 10^{th} cycle. A comparison of the first-cycle capacities with the values of the *R*-parameter shows that they have an inverse linear relationship: the lower the *R* value, the higher the capacity.

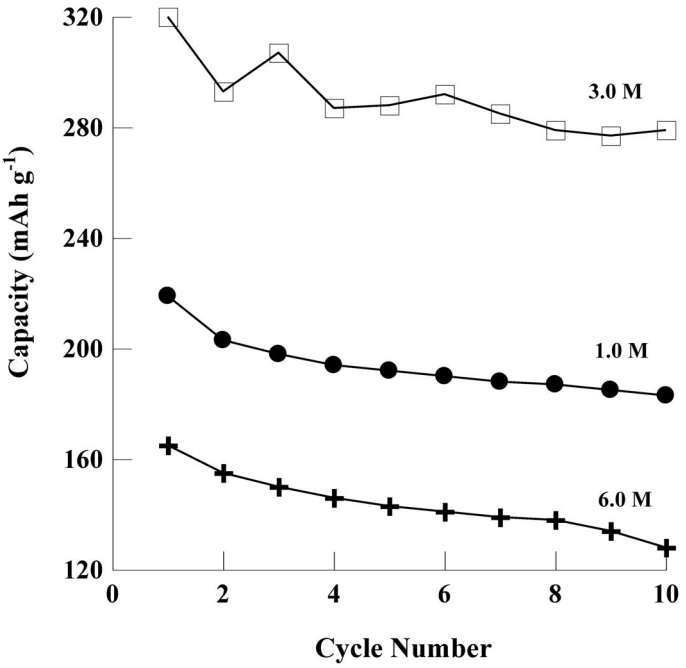

Fig. 3 Cycling behavior of carbons derived from HCl-treated rice husk.

The cycling behavior of the carbons derived from rice husk treated with NaOH is depicted in Fig. 4. The first-cycle insertion and deinsertion capacities of these carbons were, respectively, 314 and 131 mAh g^{-1} (C-N-0.01); 444 and 165 mAh g^{-1} (C-N-0.1); 819 and 463 mAh g^{-1} (C-N-0.3); 571 and 354 mAh g^{-1} (C-N-4.0); and 390 and 169 mAh g^{-1} (C-N-9.0). With the intermediate concentrations (0.3 and 4.0 M), the capacities and the coulombic efficiencies were higher. Similar to the C-H-X series carbons, the deliverable capacities of the C-N-X series carbons fell drastically with cycling. Similarly, the columbic efficiencies increased with cycling, registering 100 % in the 10^{th} cycle for the C-N-0.3 carbon. It can be seen that the capacities were roughly inversely proportional to the values of the *R*-parameter. In other words, the enhanced capacities are commensurate with the number of disoriented single layers of carbon in the materials, which provide additional sites for lithium accommodation. Obviously, an escalation in the disorderliness of the layers should effectively enhance not only the number of double surfaces available for lithium accommodation, but also the number of micropores as well. Both contribute to greater insertion and deinsertion capacities.

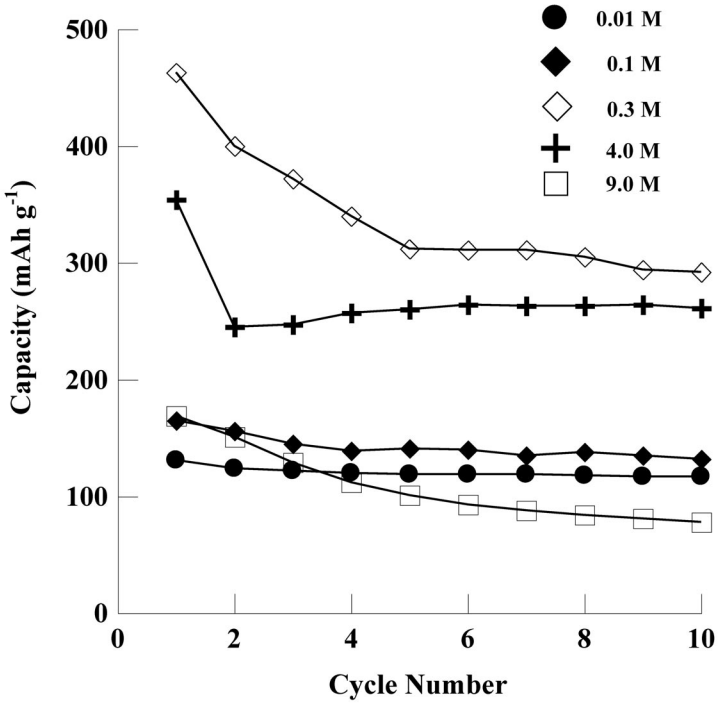

Fig. 4 Cycling behavior of carbons derived from NaOH-treated rice husk.

In general, the C-H-X and C-N-X series carbons showed initial lithium-insertion capacities of more than 372 mAh g^{-1}. It must be noted that in addition to the single-layer carbons, the hydrogen content of disordered carbons can influence their lithium-insertion capacities [45]. Incidentally, all the above carbons displayed large hysteresis in their charge–discharge curves, as observed with other hydrogen-containing carbons [4,5,45]. In the case of hydrogen-containing carbons, lithium forms a bridge with the hydrogen-containing edge carbons through an (H–C)–Li bonding [5,45]. However, Table 2 shows that as the NaOH concentration was increased, the H/C ratio of the carbons fell. Simultaneously, there was a general decrease in the *R*-parameter value and an increase in the surface area of the carbons. It appears that the cumulative effect of all these factors determined the observed capacities of the products.

CONCLUSIONS

Direct refluxing of hydrochloric acid and sodium hydroxide with rice husk and heat treatment up to 700 °C was shown to be a very good activation procedure for obtaining activated carbons with high surface areas and high micropore volume. Pyrolytic carbons obtained from rice husk treated with different concentrations of HCl or NaOH were investigated for their lithium-insertion properties. X-ray diffraction data revealed a general decrease in the interlayer spacing (d_{002}) and *R*-parameter with an increase in the concentration of the leachant. The alkali-treated rice husk yielded carbons whose H/C ratios decreased with an increase in the concentration of the alkali. An increase in the alkali concentration also led to an increase in the surface area of the carbon. The highest insertion and deinsertion capacities were observed with the carbon obtained from rice husk treated with 0.3 M NaOH, at 819 and 463 mAh g^{-1}, respectively. The capacities of all the carbons fell with cycling, although their coulombic efficiencies were as high as 100 % in the 10^{th} cycle.

ACKNOWLEDGMENTS

The National Science Council of the Republic of China and Yuen-Ze University are gratefully acknowledged for providing the financial support for carrying out this work.

REFERENCES

1. N. H. Zhao, L. J. Fu, L. C. Yang, T. Zhang, G. J. Wang, Y. P. Wu, T. van Ree. *Pure Appl. Chem.* **80**, 2283 (2008).
2. W. R. Liu, J. H. Wang, H. C. Wu, D. T. Shieh, M. H. Yang, N. L. Wu. *J. Electrochem. Soc.* **152**, A1719 (2005).
3. W. R. Liu, N. L. Wu, D. T. Shieh, H. C. Wu, M. H. Yang, C. Korepp, J. O. Besenhard, M. Winter. *J. Electrochem. Soc.* **154**, A97 (2007).
4. K. Sato, M. Noguchi, A. Demachi, N. Oki, M. Endo. *Science* **264**, 556 (1994).
5. J. R. Dahn, T. Zheng, Y. H. Liu, J. S. Xue. *Science* **270**, 590 (1995).
6. A. Mabuchi, K. Tokumitsu, H. Fujimoto, T. Kasuh. *J. Electrochem. Soc.* **142**, 1041 (1995).
7. M. Hara, A. Satoh, N. Takami, T. Ohsaki. *J. Phys. Chem.* **99**, 16338 (1995).
8. G. T. K. Fey, D. C. Lee, Y. Y. Lin. *J. Power Sources* **119–121**, 39 (2003).
9. G. T. K. Fey, C. L. Chen. *J. Power Sources* **97–98**, 47 (2001).
10. E. Peled, V. Eshkenazi, Y. Rosenberg. *J. Power Sources* **76**, 153 (1998).
11. K. E. Pappacena, S. P. Gentry, T. E. Wilkes, M. T. Johnson, S. Xie, A. Davis, K. T. Faber. *J. Eur. Ceram. Soc.* **29**, 3069 (2009).
12. G. T. K. Fey, D. C. Lee, Y. Y. Lin, T. P. Kumar. *Synth. Met.* **139**, 71 (2003).
13. W. Xing, J. S. Xue, T. Zheng, A. Gibaud, J. R. Dahn. *J. Electrochem. Soc.* **143**, 3482 (1996).
14. H. Chen, M. Armand, G. Demailly, F. Dolhem, P. Poizot, J. M. Tarascon. *Chem. Sus. Chem.* **1**, 348 (2008).
15. A. Gibaud, J. S. Xue, J. R. Dahn. *Carbon* **34**, 499 (1996).
16. G. T. K. Fey, K. L. Chen, Y. C. Chang. *Mater. Chem. Phys.* **76**, 1 (2002).
17. G. T. K. Fey, Y. C. Kao. *Mater. Chem. Phys.* **73**, 37 (2002).
18. A. Oberlin, M. Villey, A. Combaz. *Carbon* **18**, 347 (1980).
19. R. H. Bradley, B. Rand. *J. Colloid Interface Sci.* **169**, 168 (1995).
20. K. J. Masters, B. McEnaney. *Carbon* **22**, 595 (1984).
21. K. S. W. Sing, D. H. Everett, R. A. W. Haul, L. Moscou, R. A. Pierotti, J. Rouquerol, T. Siemieniewska. *Pure Appl. Chem.* **57**, 603 (1985).
22. Y. P. Wu, C. R. Wan, C. Y. Jiang, S. B. Fang, Y. Y. Jiang. *Carbon* **37**, 1901 (1999).

23. A. I. Shames, A. M. Panich, E. Mogilko, J. Grinblat, E. W. Prilutskiy, E. A. Katz. *Diamond Relat. Mater.* **16**, 2039 (2007).
24. V. Y. Osipov, T. Enoki, K. Takai, K. Takahara, M. Endo, T. Hayashi, Y. Hishiyama, Y. Kaburagi, A. Y. Vul. *Carbon* **44**, 1225 (2006).
25. Y. P. Wu, C. Jiang, C. Wan, R. Holze. *Solid State Ionics* **156**, 283 (2003).
26. K. Guerin, A. Fevrier-Bouvier, S. Flandrois, B. Simon, P. Biensan. *Electrochim. Acta* **45**, 1607 (2000).
27. E. Buiel, J. R. Dahn. *Electrochim. Acta* **45**, 121 (1999).
28. Q. Wang, H. Li, L. Q. Chen, X. J. Huang. *Solid State Ionics* **152–153**, 43 (2002).
29. T. Zheng, J. R. Dahn. *J. Power Sources* **68**, 201 (1997).
30. N. Takami, A. Satoh, T. Ohsaki, M. Kanda. *J. Electrochem. Soc.* **145**, 478 (1998).
31. T. Zheng, Y. Liu, E. W. Fuller, S. Tseng, U. von Sacken, J. R. Dahn. *J. Electrochem. Soc.* **142**, 2581 (1995).
32. R. V. Krishnarao, Y. R. Mahajan. *J. Eur. Ceram. Soc.* **15**, 1229 (1995).
33. M. Tanaka, K. Niwano, Y. Kitano. UK Patent GB 2,168,333A, 18 June (1988).
34. R. E. Franklin. *Proc. R. Soc. London*, *Ser. A* **209**, 196 (1951).
35. J. R. Dahn, A. K. Sleigh, H. Shi, J. N. Reimers, Q. Zhong, B. M. Way. *Electrochim. Acta* **38**, 1179 (1993).
36. D. F. Houstan. In *Rice Chemistry and Technology*, p. 301, American Association of Cereal Chemists, St. Paul, MN (1972).
37. R. V. Krishnarao, M. M. Godkhindi, M. Chakraborty, P. G. Mukunda. *J. Am. Ceram. Soc.* **74**, 2869 (1991).
38. Y. Liu, J. S. Xue, T. Zheng, J. R. Dahn. *Carbon* **34**, 193 (1996).
39. J. R. Dahn, W. Xing, Y. Cao. *Carbon* **35**, 825 (1997).
40. N. Takami, A. Satoh, T. Ohsaki, M. Kanda. *Electrochim. Acta* **42**, 2537 (1997).
41. J. Hayashi, A. P. Watkinson, K. C. Teo, S. Takemoto, K. Muroyama. *Coal Sci.* **1**, 1121 (1995).
42. M. J. Illan-Gomez, A. Garcia-Garcia, C. Salinas-Martinez de Lecea, A. Linares-Solano. *Energy Fuels* **10**, 1108 (1996).
43. M. A. Lillo-Rodenas, D. Lozano-Castello, D. Cazorla-Amoros, A. Linares-Solano. *Carbon* **39**, 751 (2001).
44. Y. Guo, S. Yang, K. Yu, J. Zhao, Z. Wang, H. Xu. *Mater. Chem. Phys.* **74**, 320 (2002).
45. T. Zheng, J. S. Xue, J. R. Dahn. *Chem. Mater.* **8**, 389 (1996).

